Hydroxyapatite gel for the improved removal of Pb2+ ions from aqueous solution

Doan Pham Minh, Ngoc Dung Tran, Ange Nzihou, Patrick Sharrock

Hydroxyapatite gel for the improved removal of Pb^{2+} ions from aqueous solution

Doan Pham Minh *, Ngoc Dung Tran, Ange Nzihou, Patrick Sharrock

Université de Toulouse, Mines Albi, CNRS, Centre RAPSODEE, Campus Jarlard, F-81013 Albi cedex 09, France

GRAPHICAL ABSTRACT

SEM images of Ca-HA particles: (A) Non-polished and before Pb^{2+} sorption; (B) Polished and before Pb^{2+} sorption; (C) Non-polished and after Pb^{2+} sorption; (D) Polished and after Pb^{2+} sorption.

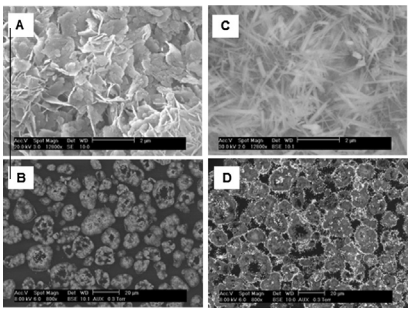

ABSTRACT

Hydroxyapatite ($Ca_{10}(PO_4)_6(OH)_2$, Ca-HA) is a versatile material which can be used in several applications. This study investigated the reactivity of Ca-HA, obtained directly by the one-step synthesis from calcium carbonate and orthophosphoric acid as low-cost initial reactants, in the removal of lead(II) as a model heavy metal. The sorption capacity of synthesized Ca-HA reached at least 750 mg g^{-1}, which was much higher than that reported in the literature. This was explained by the favorable effect of the carbonate anion presence in the apatitic structure. Classical stoichiometric lead hydroxyapatite was formed, which was found on the surface of Ca-HA particles. Small amounts of lead oxide were also detected, possibly due to a surface precipitation reaction of lead(II). The crystalline structure of the initial Ca-HA material was destroyed, in relation with the acidic conditions during the sorption experiment, as well as the insertion of lead(II) into this structure. Ionic exchange, surface complexation and dissolution–precipitation all occur and explain lead(II) fixation. The results obtained open a new pathway for the synthesis of low-cost Ca-HA sorbents for environmental purposes.

Keywords:
Calcium hydroxyapatite
Carbonated apatite
Lead
Sorption
Mechanism
Drying

1. Introduction

Heavy metals cause serious environmental concerns because of their sustained bio-toxicity. Heavy metals can be present in the environment from different anthropic sources as well as from natural geochemical processes. For example, the treatment of both municipal and industrial solid wastes by incineration technique is a major source of heavy metal emissions. Under high incineration temperatures, heavy metals present in wastes are partially or totally vaporized as a function of the nature of metals and combustion conditions. Gases emitted from incinerators require specific pollution control equipment adapted to high temperatures and complexity in terms of composition and physico-chemical properties [1,2]. In addition to anthropic sources, heavy metal contamination can also arise from natural

* Corresponding author. Tel.: +33 563493258; fax: +33 563493043.
E-mail address: doan.phamminh@mines-albi.fr (D. Pham Minh).

geochemical processes, where significant heavy metal background levels can be found in large environment areas (soil, sediment, groundwater, etc.) [3–8].

In the last decades, calcium hydroxyapatite (Ca-HA, chemical formula: $Ca_{10}(PO_4)_6(OH)_2$) was largely studied as an effective sorbent for the abatement of heavy metals under laboratory conditions, particularly in liquid phase. Because of its interesting physico-chemical properties such as low water solubility, possibility to high specific surface area, and its particular chemical structure [9,10], Ca-HA can be used for the removal of several metallic cations from aqueous solutions, for example, Cu^{2+} [11,12], Pb^{2+} [13], Zn^{2+} [12,14], Co^{2+} [15], Cd^{2+} and Ni^{2+} [16] etc. For environmental purposes, Ca-HA of low cost is required for the large scale viability of treatment processes. However, the most common method for Ca-HA synthesis is the so-called double decomposition where a calcium salt (i.e. $Ca(NO_3)_2$) reacts with an orthophosphate salt (i.e. $NH_4H_2PO_4$) under controlled pH and temperature, followed by separation and eventually washing steps. In this case, large amounts of NH_4NO_3 by-product are formed and its separation from well-dispersed Ca-HA particles is not easy. Other methods such as sol–gel synthesis [17], solid–solid reaction [18], and ultrasonic spray freeze–drying [19] have been investigated but they also present drawbacks, namely high energy cost and/or the generation of aqueous wastes and difficulties for the separation and washing step.

Our previous work was devoted to the elaboration of Ca-HA from orthophosphoric acid (H_3PO_4) and calcium carbonate ($CaCO_3$) as unconventional calcium source [20]. The results showed that Ca-HA could be obtained by the addition of concentrated orthophosphoric acid into a suspension of calcium carbonate at 80 °C, under ambient pressure for about 24 h, conditions comparable to those used for the traditional synthesis of Ca-HA from soluble calcium salts. Carbon dioxide was the only by-product which left the reaction mixture in gas form. A stable gel of finely-divided Ca-HA particles in aqueous suspension was formed, which could be used as-is, or solid Ca-HA powder could be recovered by a simple filtration or centrifugation step, without any rinsing.

In this work, we investigated the removal of soluble lead(II) as a model heavy metal from a synthetic aqueous solution using the so-called green Ca-HA, obtained from the reaction of calcium carbonate and orthophosphoric acid, mentioned above. The results obtained will help to evaluate the performance of the synthesized Ca-HA compared to the literature data. The novelty of this study is found in the use of Ca-HA under gel form which constitutes a new approach for the design of wastewater treatment processes.

2. Materials and methods

Ca-HA was synthesized according to our previous study [20]. Briefly, orthophosphoric acid (85 wt.%, p.a. grade from Merck) was pumped into an aqueous suspension of calcium carbonate ($CaCO_3$, d_{50} of 13.20 μm, >98% from Fisher Scientific) at 80 °C. The reaction mixture was kept at atmospheric pressure under 350 rpm for 24 h. A white and stable gel of fine particles was formed which contained up to 97 wt.% of Ca-HA and some traces of carbonated apatite (CAP) [20]. The gel generated by this synthetic procedure contained only trace amounts of soluble calcium and orthophosphate species [20]. A third of this gel was kept at ambient temperature in a closed glass bottle for further sorption study. This part of the gel was designated "Gel_25" thereafter. The second third of the gel was filtered on a 0.45 μm filter paper and the powder was dried overnight at 105 °C. This powder was designated "Powder_105". The last third of the gel was also filtered but the powder was dried freely at room temperature (about 25 °C) up to unchanged mass. Supplementary infra-red (FTIR) and thermogravimetry (TG) analyses were used to follow water evaporation at room temperature. The resulting powder was designated "Powder_25".

Aqueous solution of lead nitrate was prepared by dissolving lead nitrate (p.a. grade from Fisher Scientific) in permuted water for obtaining 6000 ppm (or 28.96 mmol L^{-1}) lead(II) solution. Sorption experiments were carried out in a 700 mL stirred glass reactor containing 300 mL of the prepared lead nitrate solution. The experiment started by addition of 2.4 g of powder sorbent into the reactor under regular stirring (350 rpm) at room temperature (ca. 25 °C). When Gel_25 was used as sorbent, its water content was previously determined in order to calculate the equivalent quantity compared to powder sorbents. Samples were periodically withdrawn from the reactor for the determination of the concentration of soluble lead, calcium and phosphorus by inductively coupled plasma atomic emission spectroscopy (ICP–AES). During the reaction, the pH was continuously monitored using LabView program. At the end of the sorption experiment, the solid phase was recovered by filtration and dried overnight at 105 °C for further characterizations.

Elemental analysis was carried out by ICP–AES technique on a HORIBA Jobin Yvon Ultima 2. X-ray diffraction (XRD) data were collected on a Phillips Panalytical X'pert Pro MPD diffractometer. Simultaneous thermogravimetry and differential scanning calorimetry (TG–DSC) analysis was performed in a TA Instruments SDTQ600 analyzer using an air flow rate at 100 mL min^{-1} and a heating rate of 5 °C min^{-1}. For each TG–DSC analysis, an exact weight of about 30 mg of powder was used. IR characterization was obtained on a Shimadzu FTIR 8400S spectrometer in the wavenumber range 4000–500 cm^{-1}. Specific surface area of the solid was determined by nitrogen adsorption using Micrometrics Gemini Vacprep 061 apparatus and BET equation (S_{BET}). Particle size distribution was measured by laser scattering in a Mastersizer 2000 (Malvern Instruments Ltd., Malvern, UK) in the range from 0.020 to 2000 μm. Scanning electron microscopy coupled with energy dispersive spectroscopy (SEM-EDX) was performed on a Philips XL30 ESEM apparatus (FEI Company). This apparatus is equipped with a secondary electron detector (SE mode), and a back-scattered electron (BSE) mode. SEM study was either directly carried out on the external surface of powder particles using only metallization as pre-treatment, or inside particles after embeding and mechanical polishing steps. In the last case, the immobilization of powder particles in a solid matrix of resin was carried out with a Mecaprex resin and triethylenetetramine (TETA) as hardening agent. Then, the samples were polished to fracture powder particles without damage in order to look inside.

3. Results and discussion

3.1. Lead(II) sorption

The concentration evolution of consumed lead(II) and released calcium(II) as a function of sorption time is shown in Fig. 1, where 2.4 g of Ca-HA powder or an amount of Gel_25 equivalent to 2.4 g of Ca-HA powder were set in contact with 300 mL of 6000 ppm lead(II). For these experiments, the sorbent concentration was 8.0 g L^{-1}. In all cases, lead(II) removal took place in two stages. The first stage occurred within about 60 min where about 4 mmol L^{-1} of lead(II) were removed. Lead(II) was then nearly totally removed in the second sorption stage. For Gel_25 and Powder_25 sorbents, the second stages finished before 300 min of sorption. For Powder_105 sample, a longer sorption time was required for the complete removal of lead(II) from the synthetic wastewater. In other words, the drying step at 105 °C led to a decrease in the reactivity of Ca-HA sorbent.

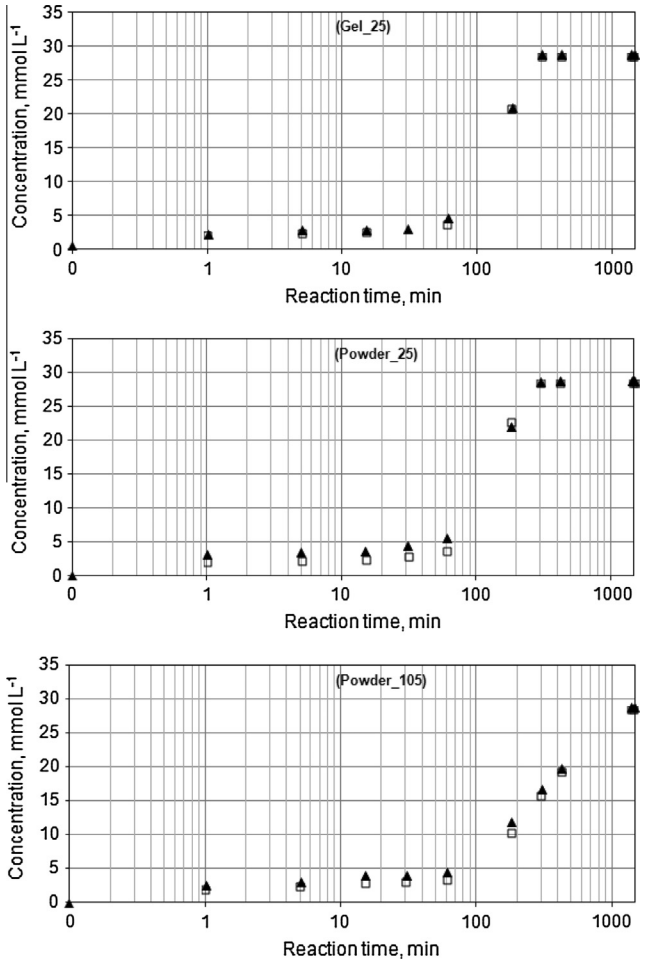

Fig. 1. Consumed Pb (□) and released Ca (▲) during the sorption of Pb using different Ca-HA sorbents: (A) Ca-HA gel; (B) Ca-HA powder dried at the ambient conditions; (C) Ca-HA powder dried at 105 °C; reaction time is in logarithm base 10 scale.

For all sorbents, the concentration of released calcium(II) was close to that of consumed lead(II) throughout the reaction time. This suggested an equimolar ionic exchange between lead(II) and calcium(II) as observed previously with other Ca-HA materials [21,22].

In order to better understand the fixation of lead(II) on Ca-HA sorbents, different physico-chemical characterizations were performed on Powder_25, Powder_105 as well as the solid recovered after sorption experiments, which are discussed in the next sections. On the other hand, Gel_25 was not characterized because the physico-chemical techniques used did not allow the study of a gel form.

3.2. XRD characterization

Fig. 2A presents XRD patterns of Powder_25 and Powder_105 which both were similar to each other. All peaks could be attributed to poorly crystallized Ca-HA phase (JCPDS standard No. 01-072-1243), as indicated by their weak broad peaks [20].

Fig. 2B shows the XRD patterns of the solid recovered after reaction with lead(II). All solids had higher crystallinity than the initials, and showed similar patterns to each other. All peaks could be attributed to lead hydroxyapatite ($Pb_{10}(PO_4)_6(OH)_2$, JCPDS standard No. 01-087-2477) and eventually some trace of lead oxide (PbO, JCPDS standard No. 01-078-1664 or 01-072-1551). Particularly, only trace amounts of poorly-crystalline Ca-HA were detected although about two-thirds of the initial Ca-HA sorbent might not participate in the sorption, taking into account the amount of removed lead(II). In fact, in these sorption experiments, the initial quantity of lead(II) in the synthetic wastewater was 8.69 mmol and the initial quantity of calcium(II) present in the sorbent of each sorption was about 24 mmol. Assuming equimolar ionic exchange as suggested by the evolution of consumed lead(II) and released calcium(II) in Fig. 1, only a third of the calcium(II) ions of the sorbents was replaced by lead(II). The decrease of visible diffractions of poorly-crystalline Ca-HA phase suggests that during sorption experiment, a destructuring of the crystalline network of the sorbents occurred. This was previously observed for the removal of lead nitrate by Ca-HA at acidic pH [21], and was attributed to the changes of interatomic distances and bond angles by the insertion of lead(II) into the structure of Ca-HA [23]. It could also be due to the loss of the broad diffraction signal for poorly crystallized Ca-HA concealed under the strong lines of the more crystalline lead hydroxyapatite.

3.3. FTIR analysis

FTIR spectra of the initial sorbents are presented in Fig. 3A. Only a weak broad peak was observed at about 3570 cm^{-1} in the wavenumber range of 4000−1700 cm^{-1}, attributed to hydroxyl groups (not presented). No evidence of the principal peak of calcite at 1389 cm^{-1} was observed because of its complete decomposition during the Ca-HA synthesis. On the other hand, a bi-modal peak at 1450/1415 cm^{-1} and single peaks at 1545, 880 and 870 cm^{-1} were observed, which are characteristic for vibrations of carbonate groups, inserted in the apatitic structure [20]. Phosphate groups of Ca-HA structure were clearly observed at about 1040, 960, 601 and 570 cm^{-1} [24].

FTIR spectra of the solids after lead(II) sorption are shown in Fig. 3B. The reaction of lead(II) with the apatitic structure of Ca-HA led to some changes of IR vibrations of functional groups. A decrease in the intensity of carbonate vibrations was observed, which might be due to the partial decarbonation when Ca-HA sorbents were in contact with acidic solution of lead(II) nitrate (initial pH of 5.1 at room temperature). The bi-modal peak at 1020/970 cm^{-1} and peaks at 601 and 570 cm^{-1} were characterized as phosphate vibrations in lead(II) substituted Ca-HA [25]. This confirmed again the presence of lead(II) phosphate together with the apatitic structure of Ca-HA as shown above by XRD results.

3.4. TG–DSC analysis

Thermal behavior of sorbents before and after sorption experiment was investigated using TG–DSC technique. Both initial Powder_25 and Powder_105 had similar TG profiles to each other (Fig. 4A). The only difference between these two sorbents was found as a higher weight loss of Powder_25 in the temperature range of 25–105 °C, compared to that of Powder_105. This was attributed to the location of free water in porous Ca-HA matrix, which could not be removed by drying at room temperature. The next weight loss in the temperature range of 105–650 °C was due to the dehydration of lattice molecular water [26]. From 650 to 1280 °C, the weight loss was attributed to the decarbonation of CO_3^{2-} groups present in Ca-HA structure [27,28]. Finally, a small net weight loss was observed at 1280–1315 °C and was attributed to the loss of OH^- groups present in apatitic network and the formation of oxyhydroxyapatite [28,29].

The solids recovered after lead(II) sorption had practically the same thermal behavior. The weight losses corresponding to the removal of both surface moisture (25–105 °C) and lattice molecular

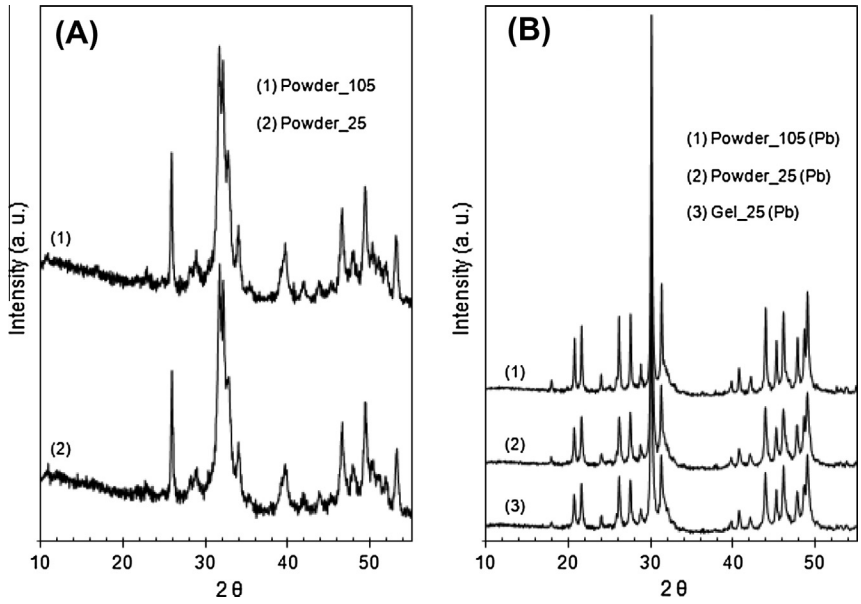

Fig. 2. XRD patterns of the solid sorbents before lead(II) sorption experiments (A); and solids recovered from lead(II) sorption experiments and dried overnight at 105 °C (B).

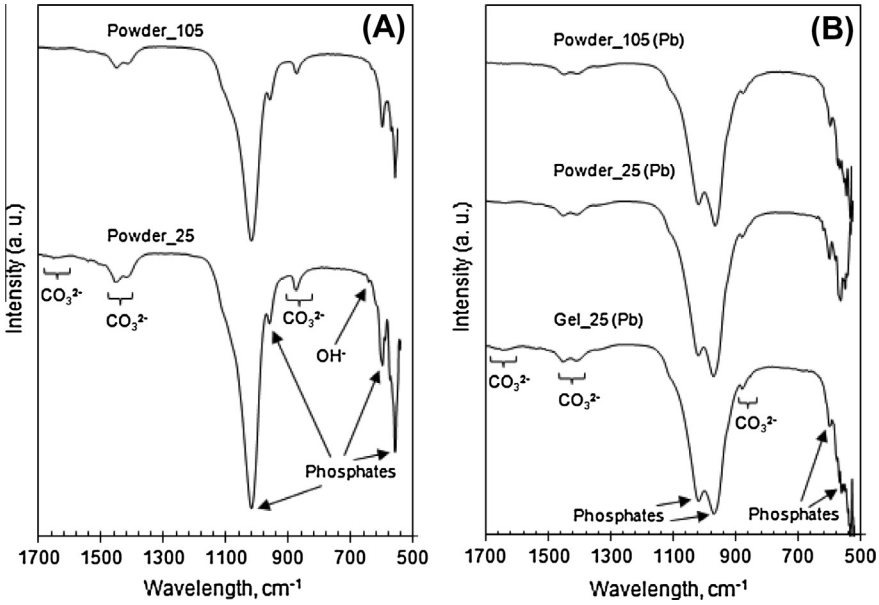

Fig. 3. FTIR spectra of the initial sorbents (A); and of the sorbents after lead(II) sorption, dried overnight at 105 °C (B).

water (105–650 °C), and the decarbonation of CAP (650–1000 °C) were proportionally smaller than those of the initial sorbents, because of the presence of lead(II), heavier than calcium(II), in the apatitic structure. Particularly, a strong weight loss starting at 850 °C was observed and it did not yet end when the temperature reached 1450 °C. At this temperature, the total weight loss was of about 44%, much higher compared to that of the initial sorbent. This could be due to evaporation of P_2O_5. This is of interest, for further study, to understand the thermal behavior of lead-doped Ca-HA, since it is used in high temperature processes, for example in the catalytic reforming of refractory molecules such as methane and butan-1-ol [25,30–32].

All weight losses mentioned above were endothermic (DSC results not presented).

3.5. SEM analysis

The morphology and external surface texture of Powder_105 is illustrated in Fig. 5. Particle sizes varied in a large range from hundreds of nm to more than 100 μm (Fig. 5A and B). At higher magnifications, it is evident that Ca-HA particles were formed by agglomeration of smaller ones (Fig. 5C). At the external surface, sheet or plate-like structure was then observed which is characteristic for Ca-HA particles [33].

Fig. 6 presents SEM images of fractured Ca-HA particles. In most of cases, hollow Ca-HA particles were observed. In addition to the porosity due to this hollowness, pores of different sizes could be also observed on the border of these hollow Ca-HA particles. This porosity is favorable for the contact of lead(II) cations with the

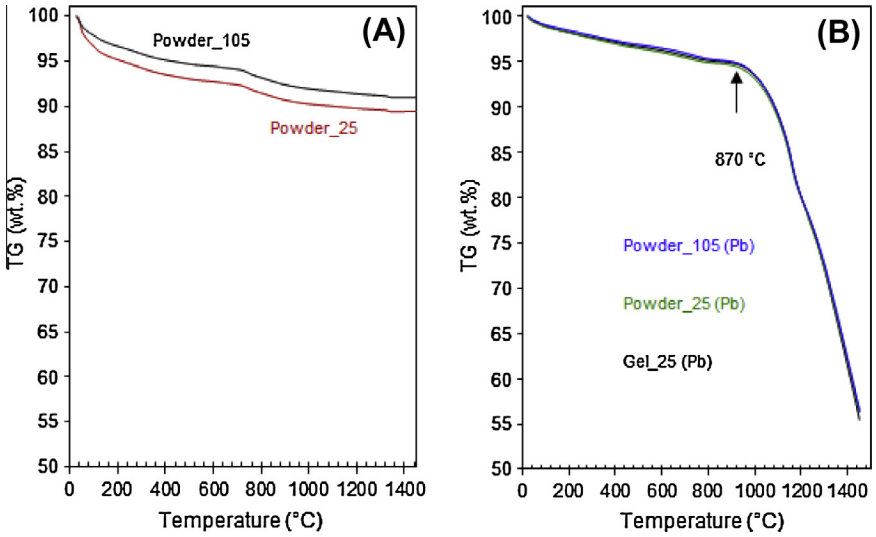

Fig. 4. TG curves of the initial sorbents (A); and of the sorbents after lead(II) sorption, dried overnight at 105 °C (B).

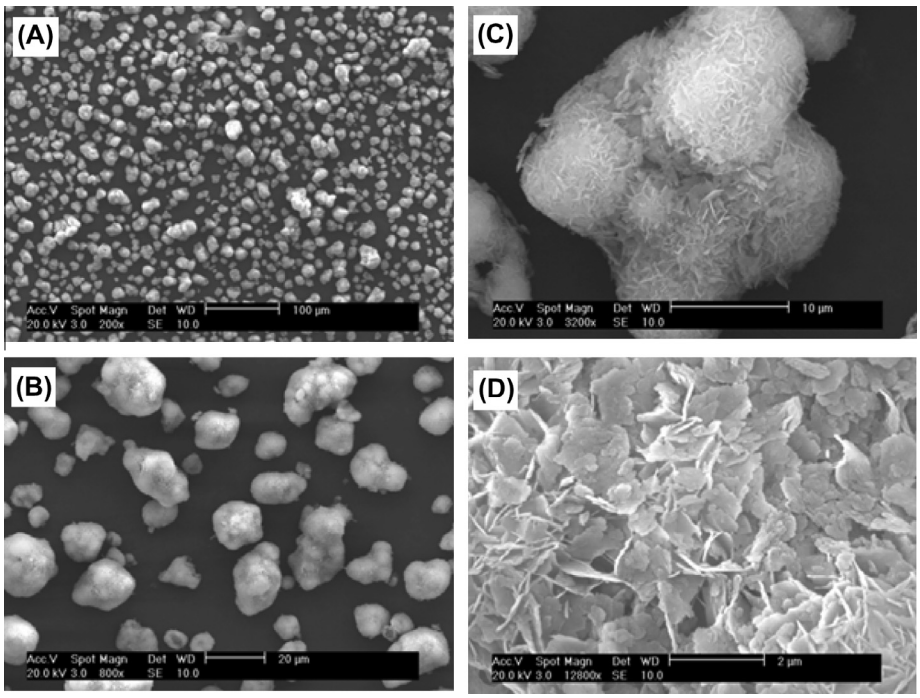

Fig. 5. SEM observation on the external surface of Powder_105 before lead(II) sorption.

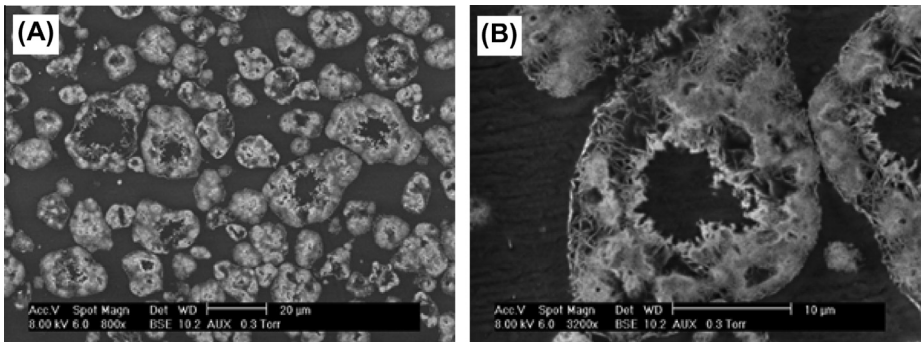

Fig. 6. SEM observation inside particles of Powder_105 before lead(II) sorption.

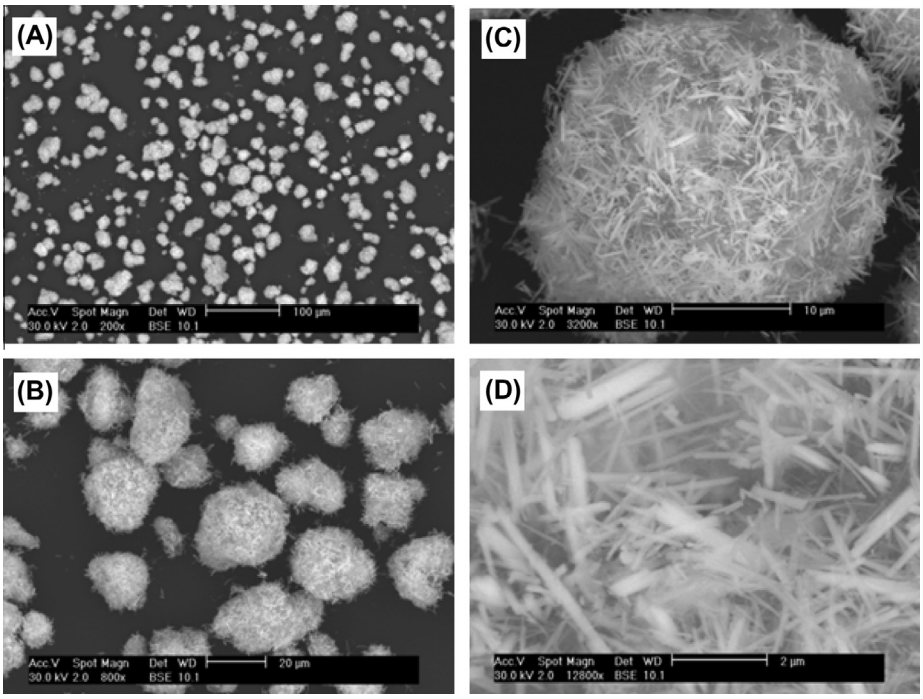

Fig. 7. SEM observation on the external surface of Powder_105 after lead(II) sorption.

sorbent surface when pores are connected to the external surface (open-porosity). Similar results were observed for Powder_25 sorbent (results not presented).

SEM images of the external surface of Powder_105 after lead(II) sorption are presented in Fig. 7. Particle sizes were apparently not changed compared to those of Powder_105 before lead(II) sorption

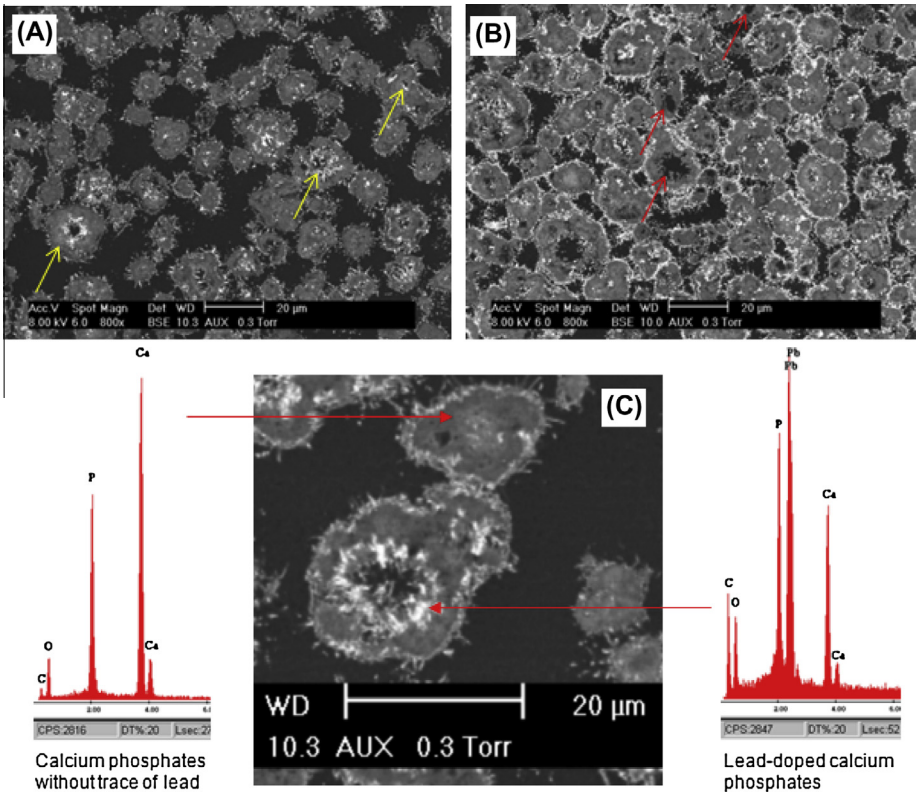

Fig. 8. SEM observation inside particles of Powder_105 after lead(II) sorption; (A) yellow arrows: open macro-porosity; (B) red arrows: closed macro-porosity. (For interpretation of the references to color in this figure legend, the reader is referred to the web version of this article.)

(Fig. 5A and B). However, the textural structure at the surface of particles was completely modified. Particles of sheet structure disappeared and new needle-like particles were abundantly formed (Fig. 7C and D). EDX analysis confirmed clearly the presence of lead on the surface of the sorbent (not shown).

In order to better observe the immobilization of lead, SEM study inside sorbent particles was carried out and the BSE images are illustrated in Fig. 8. With higher atomic number compared to those of other elements (calcium, phosphorus, oxygen), lead had the highest contrast and its presence could be distinctly observed on the surface of the sorbent, located either on the external surface of particles or surface of pores. The embeding and polishing techniques used for preparing SEM sample highlighted also the presence of both open macro-porosity (yellow arrows, Fig. 8A), where lead could get into and be immobilized, and closed macro-porosity (red arrows, Fig. 8B) where no trace of lead was observed. Several EDX analyses were repeated which confirmed the observation of BSE images, as illustrated in Fig. 8C.

Imaging of the main elements present in the used sorbent was also performed in order to have a global observation on the distribution of lead, calcium and phosphorus (Fig. 9). All images in Fig. 9 were set at the same scale. Fig. 9 A presents the BSE image from which imaging of lead, calcium and phosphorus was built by EDX analysis. Lead was present at high frequency on the external surface of particles and at lower frequency inside open-pores (Fig. 9B). On the other hand, calcium was principally observed in the underlying layers where lead could not get into (Fig. 9D). This indicated the substitution of calcium(II) by lead(II) at the accessible surface of Ca-HA particles. Phosphorus was generally present over entire sorbent particles (Fig. 9C). Image treatment shows clearly that lead distribution surrounds phosphorus (Fig. 9E) but calcium and phosphorus are superimposed (Fig. 9F). Similar SEM results were observed for Powder_25 before and after lead(II) sorption.

SEM images show that particle sizes and visible macro-porosity of sorbents seemed unchanged after lead(II) sorption. To confirm this, particle size distribution and specific surface area were measured. On Fig. 10A, the initial powder dried at 25 °C (Powder_25) presents two populations of particles of 0.2–5 μm and 5–60 μm. When the sorbent was dried at higher temperature (105 °C), the 3rd population appeared at 60–220 μm, which must be due to the agglomeration of smaller particles under thermal effect as shown in Fig. 5C. After lead(II) sorption, particle size distributions of Gaussian-type were observed for both sorbents, which were found in the particle size ranges of 6–85 μm and 7–65 μm for

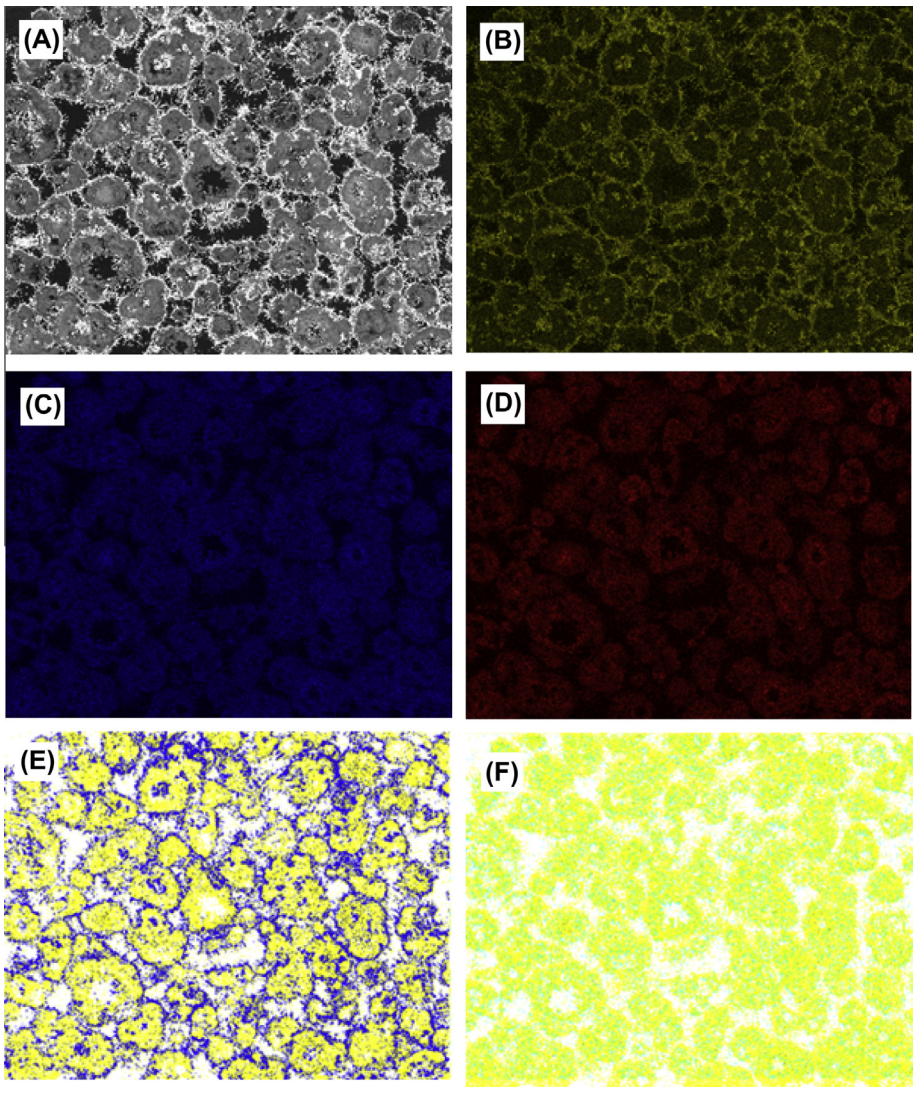

Fig. 9. Imaging of lead, calcium and phosphorus present in Powder_105 after lead(II) sorption; (A) BSE image; (B–D) imaging of lead, phosphorus and calcium, respectively; (E) image treatment of phosphorus (yellow) and lead (blue); (F) image treatment of phosphorus (yellow) and calcium (green). (For interpretation of the references to color in this figure legend, the reader is referred to the web version of this article.)

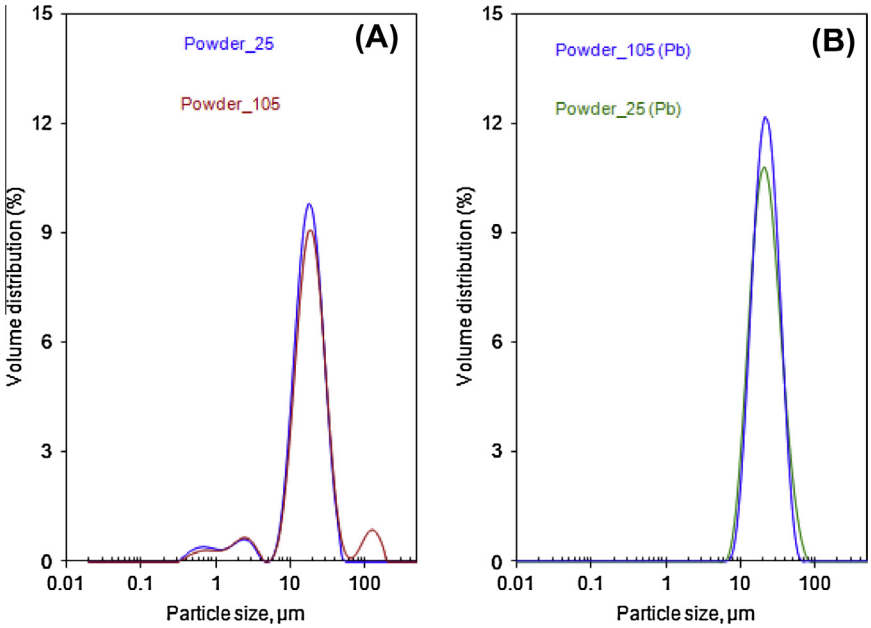

Fig. 10. Particle size distribution of the initial powder sorbents (A); and of the sorbents after lead(II) sorption, dried overnight at 105 °C (B).

Powder_25 and Powder_105, respectively. This means that particles smaller than 5 µm or larger than 85 µm in the initial sorbents were not observed after reaction. In all cases, these results were in agreement with SEM results shown above.

Specific surface areas of sorbents before and after lead(II) sorption were also measured. There was no significant change of the specific surface area after sorption compared to the initial sorbents, which were all close to ca. 40 $m^2 g^{-1}$. From ICP–AES results, the amount of released calcium was practically equal to the amount of consumed lead during sorption. The fixation of lead seemed to not change particle sizes, as well as the visible macro-porosity of the sorbent, as illustrated in Fig. 7 and Fig. 10. Thus, specific surface area was unchanged after reaction.

3.6. Discussions

3.6.1. Sorption capacity and role of carbonate anions

Using an aqueous solution containing 6000 ppm of lead(II) and the concentration of sorbent of 8.0 g L^{-1}, lead(II) was completely immobilized on Ca-HA matrix as shown in Fig. 1. This means that the quantity of lead(II) potentially retained by one gram of sorbents can reach at least 750 mg. Table 1 compares this result with those previously reported in the literature for lead(II) sorption in liquid phase.

Most literature studies reported the use of Ca-HA obtained by a precipitation method with controlled pH from soluble calcium salts. Depending on the experimental conditions of the sorption process, in particular the pH, the sorbent concentration, the initial concentration of lead(II) and the sorption time, the sorption capacity (Q_e) reported varies in the range of 104–620 mg g^{-1}. Synthetic Ca-HA is generally found to be more active than commercial Ca-HA. Under similar sorption conditions, we found that the sorbent synthesized from $CaCO_3$ and H_3PO_4 was much more active than those starting from calcium soluble salts reported in the literature. This higher activity may be due to the presence of carbonate anions remaining in the apatitic structure of our sorbent, as shown by IR results (Fig. 3). Supplementary TG–MS coupling showed that our sorbents contained approximately 2.6 wt.% of carbonate. In fact, the effect of carbonate anions on the reactivity of Ca-HA-based materials for the removal of heavy metals has been studied by Miyake et al. [37]. In this study, Ca-HA-based sorbents containing various contents of carbonate anions were synthesized from $Ca(CH_3COO)_2$ and Na_2HPO_4 in the presence of $NaHCO_3$ as carbonate source. Under the same experimental conditions, the removal of a given amount of lead(II) in an aqueous solution was completely

Table 1
Comparison of the present study with literature data.

Sorbent	Starting materials for the synthesis of sorbent	[Sorbent], g L^{-1}	[Pb], mg L^{-1}	Q_e, mg g^{-1}	Ref.
Gel_25	$CaCO_3$, H_3PO_4	8.0	6000	750[a]	This work
Powder_25	$CaCO_3$, H_3PO_4	8.0	6000	750[a]	This work
Powder_105	$CaCO_3$, H_3PO_4	8.0	6000	750[a]	This work
Ca-HA	$Ca(NO_3)_2$, $NH_4H_2PO_4$	8.0	5200	620	[34]
Ca-HA	$Ca(OH)_2$, H_3PO_4[b]	8.0	5200	104	[34]
Ca-HA	$Ca(NO_3)_2$, $(NH_4)_2HPO_4$	2.5	581–1770	470	[35]
Ca-HA	$Ca(NO_3)_2$, $(NH_4)_2HPO_4$	4.0	2072	144–426	[36]
Ca-HA	$CaCl_2$, H_3PO_4 $Ca(NO_3)_2$, $(NH_4)_2HPO_4$ $Ca(NO_3)_2$, K_2HPO_4	10.0	1000–8000	330–450	[22]
Ca-HA	$Ca(NO_3)_2$, $(NH_4)_2HPO_4$	0.2–4.0	100–400	430–700	[16]
CAP[c]	$Ca(CH_3COO)_2$, Na_2HPO_4, $NaHCO_3$	0.25	2600	1823	[37]

[a] At least.
[b] Commercial Ca-HA.
[c] Ca-HA containing 16 wt.% of carbonate.

achieved after 14 days, 4 h and 2 h when Ca-HA-based sorbents containing 0, 0.6 and 16 wt.% of carbonate were used. A very high sorption capacity of 1823 mg g^{-1} was also obtained when Ca-HA containing 16 wt.% of carbonate was used (Table 1). The effect of carbonate anions is assigned to the change in apatitic structure when carbonate anions replace orthophosphate anions for the formation of B-type carbonated apatite. For each carbonate group inserted in place of a PO_4^{3-} group, a HPO_4^{2-} group is required for the charge balance in the apatitic structure. This leads to a destabilization of apatitic structure which favors the immobilization of lead(II) [37]. Carbonated apatite (CAP) may also be less stable under acidic conditions and carbonate groups may be leached. When CAP containing high carbonate content (16 wt.%) was used, a small amount of lead carbonate could be detected by XRD and IR analysis [37].

3.6.2. About the mechanism for lead(II) fixation

Much work has been carried out on the fixation of lead(II) using apatitic sorbents and different mechanisms have been developed. The first one calls for the dissolution of Ca-HA followed by precipitation of lead hydroxyapatite or co-precipitation of lead-doped Ca-HA [22,38,39]. In our case, the precipitation of lead is supported by the formation of $Pb_{10}(PO_4)_6(OH)_2$ as shown by XRD results. However, no XRD evidence of lead-doped Ca-HA exists in the analysis of samples derived at room temperature. SEM images (Fig. 8 and 9) enhanced this hypothesis. The layer thickness of lead-rich phase was estimated at µm scale, as a result of the precipitation step. However, because the size and the visible macro-porosity and the specific surface area of sorbent particles were practically similar before and after lead(II) removal, complete dissolution of Ca-HA particles did not occur, as confirmed by BSE images. So, a dissolution–precipitation mechanism could occur partly at the surface of sorbent particles.

The second mechanism consists of the ionic exchange between calcium(II) and lead(II) [21,34,37]. Most authors announced this mechanism based on the molar ratio of released calcium(II) to removed lead(II) close to unity. Suzuki et al. [21] indicated a long exchange time under room conditions for the fixation of lead(II) by this way. Thus, the results in Fig. 1 demonstrate the possibility of ionic exchange. However, it should be emphasized that ionic exchange is not a sorption but an exchange reaction where lead displaces calcium and the end product is different from the starting one. Thus, it cannot contribute to a sorption isotherm.

In addition to these two mechanisms, lead(II) fixation at the beginning of the reaction may occur by a fast surface complexation of lead(II) on ≡POH sites [22,35,40,41]. This is supported by the continuous monitoring of pH during sorption (Fig. 11), wherein the pH decreased during the first 30 s according to Eq. (1). This pH decrease might also be explained by the presence of calcium phosphates having molar ratios of Ca/P smaller than 1.67, such as octocalcium phosphate pentahydrate ($Ca_8(HPO_4)_2(PO_4)_4{\cdot}5H_2O$), brushite ($CaHPO_4{\cdot}2H_2O$), monetite ($CaHPO_4$), or hydrated Ca-HA surfaces containing such hydrogenphosphate species, according to Eqs. (2)–(4).

$$2[\equiv POH] + Pb^{2+} \rightarrow [\equiv PO^-]_2Pb + 2H^+ \quad (1)$$

$$Ca_8(HPO_4)_2(PO_4)_4 \cdot 5H_2O + 10Pb^{2+} \rightarrow Pb_{10}(PO_4)_6(OH)_2 + 8Ca^{2+} + 2H^+ + 5H_2O \quad (2)$$

$$6[CaHPO_4 \cdot 2H_2O] + 10Pb^{2+} \rightarrow Pb_{10}(PO_4)_6(OH)_2 + 6Ca^{2+} + 8H^+ + 10H_2O \quad (3)$$

$$6CaHPO_4 + 2H_2O + 10Pb^{2+} \rightarrow Pb_{10}(PO_4)_6(OH)_2 + 6Ca^{2+} + 8H^+ \quad (4)$$

After this first short decrease, the pH increased slightly up to about 10 min, then decreased strongly between 10 and 140–180 min of contact. This might correspond to the dissolution (pH increase)–precipitation (pH decrease) phenomenon, but also to a surface precipitation of lead(II). After the first min of contact, particles of sorbents were covered by some amounts of lead(II) at the surface, which might have some catalytic nucleating effect for the surface precipitation of free lead(II) cations, present in the reaction mixture at high concentration (Eq. (5)) [42]. This hypothesis was enhanced by the detection of lead oxide at small amounts by XRD analysis.

$$Pb^{2+} + 2OH^- \rightarrow PbO + H_2O \quad (5)$$

Finally, the pH increased progressively up to 24 h of reaction, because of the buffering capacity of Ca-HA, and according to the surface property of lead-doped Ca-HA which has the point of zero charge (pHpzc) in the range of 5–6 [43].

In summary, different reactions are involved for the removal of lead(II) using such Ca-HA sorbents. The molar ratio of released calcium(II) to removed lead(II) close to unity and the decrease of pH at the beginning of the reaction suggest the preliminary fast surface complexation mechanism, leading to ionic proton-Pb^{2+} exchange. However, the destruction of the crystalline structure of Ca-HA particles, the formation of a lead-rich layer including $Pb_{10}(PO_4)_6(OH)_2$, and trace amounts of PbO on the surface of sorbent particles with layer thickness at µm scale suggest that dissolution–precipitation occurs simultaneously, particularly

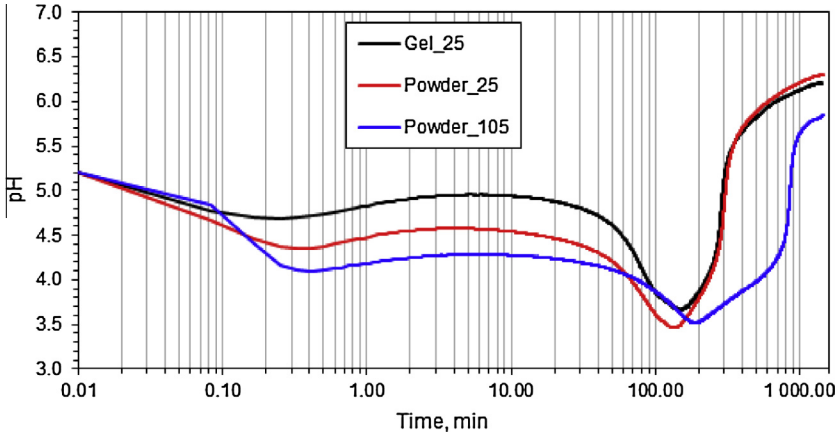

Fig. 11. pH evolution during lead(II) sorption using different Ca-HA.

under acidic initial conditions when Ca-HA is not very stable as solid phase.

3.6.3. Effect of drying temperature

The sorption results in Fig. 1 show that the drying step at 105 °C led to lower reactivity of the sorbent compared to drying at 25 °C. Firstly, this effect could be attributed to the formation of large Ca-HA particles of 60–220 μm (Fig. 10A). The removal of water at 105 °C might also lead to a lower permeability of Ca-HA. These all can perturb the diffusion of lead(II) into pores and/or lattices of Ca-HA for fixation. The inhibition by thermal treatment of the reactivity of Ca-HA for lead(II) removal was also observed by Sugiyama et al. [36] and Hadioui et al. [44].

4. Conclusions

Calcium hydroxyapatite (Ca-HA) obtained by the one-step synthesis method from calcium carbonate and orthophosphoric acid as economical starting materials at moderate conditions (80 °C, atmospheric pressure) was found to be very efficient for the removal of lead(II) as model heavy metal from an aqueous solution. No counter-ions were present in the final suspension of Ca-HA which could be directly used in gel form for lead(II) removal. In addition, the presence of carbonate anions in the apatitic structure favored the removal of lead(II) which explains the higher sorption capacity of Ca-HA synthesized in this study compared to literature data. Ca-HA particles in suspension form or dried at ambient conditions were found to be more active than Ca-HA particles dried at 105 °C which reveals the importance of the non-stoichiometric hydrated surface composition. Lead(II) was mostly immobilized on the surface of sorbent particles (external surface and pore surface) as highlighted by SEM study.

Further study will focus on the improvement of the sorption capacity of Ca-HA. A reflux of carbonic gas formed from the decarbonation of calcium carbonate to the reaction mixture may increase the carbonate content in Ca-HA sorbent, since it favors the fixation of lead(II). Synthesis conditions will be improved for obtaining smaller particles, which should further improve the fixation of lead(II).

It is also interesting to investigate the thermal behavior of lead-doped hydroxyapatite since it can be used in different high-temperature processes, such as in heterogeneous catalysis.

Acknowledgments

The authors thank gratefully Christine Rolland and Nathalie Lyczko for technical help.

References

[1] P.T. Williams, Pollutants from incineration: an overview, in: R.E. Hester, R.M. Harrison (Eds.), Waste Incineration and the Environment, Issues in Environmental Science and Technology, vol. 2, Thomas Graham House, Science Park, Cambridge, UK, 1994.
[2] S. Rio, C. Verwilghen, J. Ramaroson, A. Nzihou, P. Sharrock, Heavy metal vaporization and abatement during thermal treatment of modified wastes, J. Hazard. Mat. 148 (2007) 521–528.
[3] M.F. Horst, Heavy metal distribution in sediments and ecological risk assessment: the role of diagenetic processes in reducing metal toxicity in bottom sediments, Environ. Pollut. 97 (1997) 317–325.
[4] J.R. Miller, The role of fluvial geomorphic processes in the dispersal of heavy metals from mine sites, J. Geochem. Explor. 58 (1997) 101–118.
[5] W.C. Malcolm, D. McConchie, D.W. Lewis, P. Saenger, Redox stratification and heavy metal partitioning in Avicennia-dominated mangrove sediments: a geochemical model, Chem. Geol. 149 (1998) 147–171.
[6] A. Navas, H. Lindhorfer, Geochemical speciation of heavy metals in semiarid soils of the central Ebro Valley (Spain), Environ. Int. 29 (2003) 61–68.
[7] B. Van der Grift, J. Griffioen, Modelling assessment of regional groundwater contamination due to historic smelter emissions of heavy metals, J. Contam. Hydrol. 96 (2008) 48–68.
[8] M.A. Hashim, S. Mukhopadhyay, J.N. Sahu, B. Sengupta, Remediation technologies for heavy metal contaminated groundwater, J. Environ. Manage. 92 (2011) 2355–2388.
[9] C. Verwilghen, S. Rio, A. Nzihou, D. Gauthier, G. Flamant, P. Sharrock, Preparation of high specific surface area hydroxyapatite for environmental applications, J. Mater. Sci. 42 (2007) 6062–6066.
[10] M.I. Kay, R.A. Young, A.S. Posner, Crystal structure of hydroxyapatite, Nature 204 (1964) 1050–1052.
[11] M. Sljivic, I. Smiciklas, I. Plecas, M. Mitric, The influence of equilibration conditions and hydroxyapatite physico-chemical properties onto retention of Cu^{2+} ions, Chem. Eng. J. 148 (2009) 80–88.
[12] A. Corami, S. Mignardi, V. Ferrini, Copper and zinc decontamination from single- and binary-metal solutions using hydroxyapatite, J. Hazard. Mater. 146 (2007) 164–170.
[13] D. Pham Minh, H. Sebei, A. Nzihou, P. Sharrock, Apatitic calcium phosphates: synthesis, characterization and reactivity in the removal of lead(II) from aqueous solution, Chem. Eng. J. 198–199 (2012) 180–190.
[14] R.R. Sheha, Sorption behavior of Zn(II) ions on synthesized hydroxyapatites, J. Colloid Interf. Sci. 310 (2007) 18–26.
[15] I. Smiciklas, S. Dimovic, I. Plecas, M. Mitric, Removal of Co^{2+} from aqueous solutions by hydroxyapatite, Water Res. 40 (2006) 2267–2274.
[16] I. Mobasherpour, E. Salahi, M. Pazouki, Comparative of the removal of Pb^{2+}, Cd^{2+} and Ni^{2+} by nano crystallite hydroxyapatite from aqueous solutions: adsorption isotherm study, Arab. J. Chem. 5 (2012) 439–446.
[17] T.K. Anee, M. Ashok, M. Palanichamy, S.N. Kalkura, A novel technique to synthesize hydroxyapatite at low temperature, Mater. Chem. Phys. 80 (2003) 725–730.
[18] C.C. Silva, A.G. Pinheiro, M.A.R. Miranda, J.C. Goes, A.S.B. Sombra, Structural properties of hydroxyapatite obtained by mechanosynthesis, Solid State Sci. 5 (2003) 553–558.
[19] K. Itatani, K. Iwafune, F.S. Howell, M. Aizawa, Preparation of various calcium-phosphate powders by ultrasonic spray freeze-drying technique, Mater. Res. Bull. 35 (2000) 575–585.
[20] D. Pham Minh, N.D. Tran, A. Nzihou, P. Sharrock, One-step synthesis of calcium hydroxyapatite from calcium carbonate and orthophosphoric acid under moderate conditions, Ind. Eng. Chem. Res. 52 (2013) 1439–1447.
[21] T. Suzuki, K. Ishigaki, M. Miyake, Synthetic hydroxyapatites as inorganic cation exchangers. Part 3. Exchange characteristics of lead ions (Pb^{2+}), J. Chem. Soc. Faraday Trans. I (80) (1984) 3157–3165.
[22] S. Bailliez, A. Nzihou, D. Bernache-Assolant, E. Champion, P. Sharrock, Removal of aqueous lead ions by hydroxyapatites: equilibria and kinetic processes, J. Hazard. Mater. A139 (2007) 443–446.
[23] M. Miyake, K. Ishigaki, T. Suzuki, Structure refinements of Pb^{2+} ion-exchanged apatites by X-ray powder pattern-fitting, J. Solid State Chem. 61 (1986) 230–235.
[24] J.C. Elliott, Studies in Inorganic Chemistry 18: Structure and Chemistry of the Apatites and Other Calcium Orthophosphates, Elsevier, Amsterdam–London–New York–Tokyo, 1994.
[25] J.H. Park, D.W. Lee, S.W. Im, Y.H. Lee, D.J. Suh, K.W. Jun, K.Y. Lee, Oxidative coupling of methane using non-stoichiometric lead hydroxyapatite catalyst mixtures, Fuel 94 (2012) 433–439.
[26] W.L. Suchanek, P. Shuk, K. Byrappa, R.E. Riman, K.S. TenHuisen, V.F. Janas, Mechanochemical–hydrothermal synthesis of carbonated apatite powders at room temperature, Biomaterials 23 (2002) 699–710.
[27] W.L. Suchanek, K. Byrappa, P. Shuk, R.E. Riman, V.F. Janas, K.S. TenHuisen, Mechanochemical–hydrothermal synthesis of calcium phosphate powders with coupled magnesium and carbonate substitution, J. Solid State Chem. 177 (2004) 793–799.
[28] J.P. Lafon, E. Champion, D. Bernache-Assollant, R. Gibert, A.M. Danna, Thermal decomposition of carbonated calcium phosphate apatites, J. Therm. Anal. Calor. 72 (2003) 1127–1134.
[29] C.J. Liao, F.H. Lin, K.S. Chen, J.S. Sun, Thermal decomposition and reconstitution of hydroxyapatite in air atmosphere, Biomaterials 20 (1999) 1807–1813.
[30] T.J. Park, D.J. Suh, K.Y. Lee, Preparation of Pb-substituted hydroxyapatite catalyst and use in oxidative coupling of methane, US Patent Number 5877387, March 2, 1999.
[31] S.H. Lee, K.J. Yoon, Oxidative coupling of methane over transition-metal-substituted strontium hydroxyapatite, Korean J. Chem. Eng. 18 (2001) 228–232.
[32] Z. Boukha, M. Kacimi, M. Ziyad, A. Ensuque, F. Bozon-Verduraz, Comparative study of catalytic activity of Pd loaded hydroxyapatite and fluoroapatite in butan-2-ol conversion and methane oxidation, J. Mol. Catal. A: Chem. 270 (2007) 205–213.
[33] D. Pham Minh, N. Lyczko, H. Sebei, A. Nzihou, P. Sharrock, Synthesis of calcium hydroxyapatite from calcium carbonate and different orthophosphate sources: a comparative study, Mater. Sci. Eng. B 177 (2012) 1080–1089.
[34] I.L. Shashkova, A.I. Ratko, N.V. Kitikova, Removal of heavy metal ions from aqueous solutions by alkaline-earth metal phosphates, Colloids Surf. A: Physicochem. Eng. Aspects 160 (1999) 207–215.
[35] E. Mavropoulos, A.M. Rossi, A.M. Costa, C.A. Perez, J.C. Moreira, M. Saldanha, Studies on the mechanisms of lead immobilization by hydroxyapatite, Environ. Sci. Technol. 36 (2002) 1625–1629.
[36] S. Sugiyama, T. Ichii, H. Matsumoto, H. Hayashi, Effect of calcination and sieving of calcium hydroxyapatite on ion-exchangeability with lead cation in the presence and absence of HCl, Adv. Environ. Res. 6 (2002) 285–289.

[37] M. Miyake, K. Watanabe, Y. Nagayama, H. Nagasawa, T. Suzuki, Synthetic carbonate apatites as inorganic cation exchangers: exchange characteristics for toxic ions, J. Chem. Soc. Faraday Trans. 86 (1990) 2303–2306.
[38] X.B. Chen, J.V. Wright, J.L. Conca, L.M. Peurrung, Effects of pH on heavy metal sorption on mineral apatite, Environ. Sci. Technol 31 (1997) 624–631.
[39] H.Y. Xu, L. Yang, P. Wang, Y. Liu, M.S. Peng, Kinetic research on the sorption of aqueous lead by synthetic carbonate hydroxyapatite, J. Environ. Manage. 86 (2008) 319–328.
[40] E. Deydier, R. Guilet, P. Sharrock, Beneficial use of meat and bone meal combustion residue: ‘‘an efficient low cost material to remove lead from aqueous effluent’’, J. Hazard. Mater. 101 (2003) 55–64.
[41] E. Deydier, R. Guilet, S. Sarda, P. Sharrock, Physical and chemical characterisation of crude meat and bone meal combustion residue: ‘‘waste or raw material?’’, J. Hazard. Mater. 121 (2005) 141–148.
[42] W. Kwestroo, J. Jonge, P.H.G.M. Vromans, Influence of impurities on the formation of red and yellow PbO, J. Inorg. Nucl. Chem. 29 (1967) 39–44.
[43] I. Smiciklas, A. Onjia, S. Raicevic, Đ. Janackovic, M. Mitric, Factors influencing the removal of divalent cations by hydroxyapatite, J. Hazard. Mater. 152 (2008) 876–884.
[44] M. Hadioui, P. Sharrock, M.O. Mecherri, V. Brumas, M. Fiallo, Reaction of lead ions with hydroxylapatite granules, Chem. Pap. 62 (2008) 516–521.